

# Two Dipolar $\alpha$ -Helices within Hormone-encoding Regions of Proglucagon Are Sorting Signals to the Regulated Secretory Pathway\*

Received for publication, March 10, 2014. Published, JBC Papers in Press, April 11, 2014, DOI 10.1074/jbc.M114.563684

Leonardo Guizzetti<sup>†</sup>, Rebecca McGirr<sup>§</sup>, and Savita Dhanvantari<sup>†,§,¶,||</sup>

From the Departments of <sup>†</sup>Medical Biophysics, <sup>¶</sup>Pathology, and <sup>||</sup>Medicine, University of Western Ontario, London, Ontario N6A 3K7 and the <sup>§</sup>Metabolism/Diabetes and Imaging Programs, Lawson Health Research Institute, London, Ontario N6A 4V2, Canada

**Background:** The constituent peptides of proglucagon contain  $\alpha$ -helices that may target proglucagon to secretory granules.

**Results:** Sorting of proglucagon processing intermediates is context-dependent, despite containing two sorted domains of glucagon and glucagon-like peptide 1.

**Conclusion:** Proglucagon sorting is directed by two dipolar  $\alpha$ -helices within glucagon and GLP-1.

**Significance:** Hormone domains, rather than disordered prodomains, encode proglucagon sorting signals.

Proglucagon is expressed in pancreatic  $\alpha$  cells, intestinal L cells, and some hypothalamic and brainstem neurons. Tissue-specific processing of proglucagon yields three major peptide hormones as follows: glucagon in the  $\alpha$  cells and glucagon-like peptides (GLP)-1 and -2 in the L cells and neurons. Efficient sorting and packaging into the secretory granules of the regulated secretory pathway in each cell type are required for nutrient-regulated secretion of these proglucagon-derived peptides. Our previous work suggested that proglucagon is directed into granules by intrinsic sorting signals after initial processing to glicentin and major proglucagon fragment (McGirr, R., Guizzetti, L., and Dhanvantari, S. (2013) *J. Endocrinol.* 217, 229–240), leading to the hypothesis that sorting signals may be present in multiple domains. In the present study, we show that the  $\alpha$ -helices within glucagon and GLP-1, but not GLP-2, act as sorting signals by efficiently directing a heterologous secretory protein to the regulated secretory pathway. Biophysical characterization of these peptides revealed that glucagon and GLP-1 each encode a nonamphipathic, dipolar  $\alpha$ -helix, whereas the helix in GLP-2 is not dipolar. Surprisingly, glicentin and major proglucagon fragment were sorted with different efficiencies, thus providing evidence that proglucagon is first sorted to granules prior to processing. In contrast to many other prohormones in which sorting is directed by ordered prodomains, the sorting determinants of proglucagon lie within the ordered hormone domains of glucagon and GLP-1, illustrating that each prohormone has its own sorting “signature.”

Proglucagon is an endocrine prohormone that is expressed in pancreatic  $\alpha$  cells, intestinal L cells, and select neurons of the hypothalamus and brainstem. It is the precursor for the peptide hormones glucagon, glucagon-like peptides (GLP)-1 and

GLP-2. Glucagon is the main glucose counter-regulatory hormone, principally stimulating hepatic gluconeogenesis and glycogenolysis to maintain euglycemia (1). Conversely, GLP-1 and GLP-2 are secreted from intestinal L cells in response to nutrient ingestion; GLP-1 stimulates insulin secretion in a glucose-dependent manner, and GLP-2 increases intestinal blood flow and nutrient absorption (2). Oxyntomodulin, which contains the sequence of glucagon plus a 6-amino acid C-terminal extension (Fig. 1), is also postprandially secreted from L cells and acts as a potent appetite suppressant (3). Therefore, all three hormones exert distinct metabolic actions to maintain nutrient homeostasis.

The post-translational processing of proglucagon by prohormone convertases follows a strict temporal sequence, in which an initial cleavage at K70R71 yields two fragments, glicentin and major proglucagon fragment (MPGF),<sup>2</sup> in both  $\alpha$  cells and L cells (Fig. 1) (4, 5). Pancreatic  $\alpha$  cells produce glucagon through cleavage of glicentin by PC2 (4, 6), and PC1/3-mediated processing yields glicentin, oxyntomodulin, GLP-1, and GLP-2 within L cells and neurons (7–9). There is evidence that proglucagon processing in  $\alpha$  cells is altered under conditions of  $\beta$  cell injury such that bioactive GLP-1 is produced (10). Each of these peptide hormones must be stored in dense-core secretory granules, a compartment unique to endocrine and neuroendocrine cells, for nutrient-regulated secretion. It is well documented by pulse-chase and immunoelectron microscopy studies that the final stages of processing occur in the secretory granules (5, 11, 12), and therefore, the sorting of proglucagon to secretory granules is essential for the production of its bioactive peptide hormones. However, it is not known if the initial cleavage of proglucagon to glicentin and MPGF occurs before or after sorting to granules. One component of a sorting mechanism that appears to be common to a number of prohormones is a sorting signal that is contained within the prohormone

\* This work was supported by a Discovery Grant from the Natural Sciences and Engineering Research Council of Canada, the Lawson Health Research Institute Internal Research Fund, and an Early Researcher Award from the Ontario Ministry of Research and Innovation.

<sup>†</sup> To whom correspondence should be addressed: Lawson Health Research Institute, 268 Grosvenor St., London, Ontario N6A 4V2, Canada. E-mail: sdhanvan@uwo.ca.

<sup>2</sup> The abbreviations used are: MPGF, major proglucagon fragment; PGDP, proglucagon-derived peptide; CPE, carboxypeptidase E; CgA, chromogranin A; pro-CART, pro-cocaine and amphetamine-regulated transcript; GRPP, glicentin-related pancreatic polypeptide; PCC, Pearson's correlation coefficient.

## Proglucagon Is Sorted by Dipolar $\alpha$ -Helices

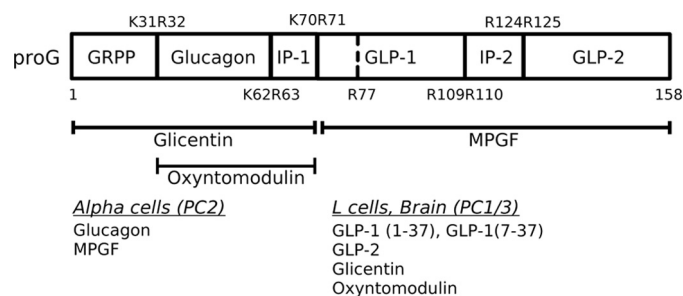


**FIGURE 1. Post-translational processing of proglucagon to its derived peptides.** Numbers indicate amino acid positions relative to proglucagon, beginning at the N-terminal amino acid. The *top* and *bottom* rows represent processing sites and removal of spacer amino acids between peptides. Major hormone products produced from tissue-specific processing by prohormone convertases are shown at *bottom*. GRPP, glicentin-related pancreatic polypeptide; IP, intervening peptide; GLP, glucagon-like peptide; MPGF, major proglucagon fragment; PC, prohormone convertase.

sequence. If the initial processing of proglucagon precedes sorting to granules, then a sorting signal must be present in each of glicentin and MPGF, leading to the intriguing possibility that proglucagon contains at least two sorting signals that are spatially segregated.

Several types of prohormone sorting signals have been described that mediate specific interactions with membrane-bound sorting receptors or co-target with processing enzymes. Proinsulin (13, 14) undergoes aggregation mediated by hydrophobic residues. A disulfide-bonded loop exposes two acidic amino acid residues comprising a sorting signal within pro-opiomelanocortin (15, 16), proinsulin (14), proenkephalin (17), and pro-brain-derived neurotrophic factor (18) and interacts with the sorting receptor carboxypeptidase E (CPE). Paired basic amino acids that are cleavage sites for prohormone convertases serve as sorting signals in pro-neuropeptide Y (19), pro-renin (20), progastrin (21), pro-neurotensin (22) and pro-VGF (nonacronymic) (23), suggesting that these prohormones are co-targeted with their processing enzymes. Finally, amphipathic  $\alpha$ -helix regions/domains are required for the sorting of pro-somatostatin (24) and pro-cocaine and amphetamine-regulated transcript (pro-CART) (25). Any or all of these sorting signals may exist within a single prohormone and may synergize to increase sorting efficiency (23, 26, 27).

Of these various known sorting signals, proglucagon contains two predicted types, significant  $\alpha$ -helical content within glucagon, GLP-1 and GLP-2, as documented by their known crystal or NMR structures (28–30) and a dibasic amino acid sequence within the  $\alpha$ -helix of glucagon ( $^{17}\text{RR}^{18}$ ; proglucagon (49–50)). Interestingly, unlike other prohormones, the  $\alpha$ -helices lie within ordered hormone-encoding regions and not in a prodomain (31). Additionally, these hormone domains are evolutionarily conserved, particularly regarding their biophysical characteristics (32). We have previously identified  $^{17}\text{RR}^{18}$  and the  $\alpha$ -helix within glucagon as putative sorting signals, and our results also suggest that processing of proglucagon to glicentin and MPGF precedes sorting (33). Therefore, in this study, we investigated the possibility that proglucagon contains multiple sorting signals in the different hormone domains. To this end, we have extensively characterized the role of each predicted  $\alpha$ -helix within proglucagon in sorting to the regulated secretory pathway in the well characterized neuroendocrine PC12 cell line. Our study reveals that two nonamphipathic  $\alpha$ -helix domains within the sequences of glucagon and GLP-1 are necessary and sufficient to target proglucagon to granules. We also combine these results to a model of proglucagon processing and sorting in  $\alpha$  and L cells.

### EXPERIMENTAL PROCEDURES

**Plasmid Construction and Reagents**—Fusion proteins were constructed using proglucagon-derived peptide sequences attached to the 3' end of the cDNA encoding the CH2/CH3 domains of mouse IgG-2b (termed Fc), preceded by the prorenin signal peptide (a kind gift from Dr. T. Reudelhuber, Montreal, Quebec, Canada) (Fig. 2), as described previously (24). Proglucagon-derived DNA sequences were amplified from Syrian hamster pre-proglucagon cDNA (a kind gift from Dr. D. Steiner, Chicago; GenBank<sup>TM</sup> accession J00059.1). All primers

were purchased from Sigma, and the specific primers used in this study for PCR amplification or site-directed mutagenesis can be found in Table 1. All fusion constructs were constructed in pcDNA3.1 (Invitrogen).

The cDNA sequence of Fc was selectively amplified using the Fc primers (Table 1) and ligated to the pcDNA3.1 backbone, between HindIII and BamHI restriction sites. To construct an Fc expression plasmid, an in-frame stop codon was mutated between the coding region and the HindIII restriction site, using the Fc stop primers (Table 1). Mutagenesis reactions were performed using the QuikChange II site-directed mutagenesis kit (Agilent Technologies, Mississauga, Ontario, Canada) according to the manufacturer's protocol.

The Fc-wild-type glucagon fusion construct was generated ("Fc-WT glucagon"; Fig. 2), in which glucagon cDNA was amplified using specific primers for glucagon (Table 1), ligated between the EcoRI and NotI restriction sites, and joined by a 10-amino acid linker (Table 1). To determine possible sorting signals, the sequence of glucagon was mutated in two ways (Fig. 2) as follows: two leucines, Leu-14 and Leu-26, which are postulated to stabilize the  $\alpha$ -helix, were mutated to L14P, L26P ("Fc-LP glucagon") by specific amplification and mutation using the respective L14P and L26P glucagon primers (Table 1); and the dibasic sequence R18R19 was changed to R18R19Q ("Fc-RQ glucagon") using the R18Q mutagenesis primers (Table 1).

Subsequent proglucagon-derived peptide constructs used a similar Fc expression system, in which Fc was ligated into the NheI and HindIII restriction sites. Expression constructs were generated for the following peptides, GLP-1(1–37), GLP-1(7–37), GLP-2, oxyntomodulin, glicentin, and MPGF (referred to as Fc-GLP-1(1–37), Fc-GLP-1(7–37), Fc-GLP-2, Fc-OXM, Fc-glicentin and Fc-MPGF, respectively; Figs. 1 and 2), and ligated into the BamHI and EcoRI restriction sites. An internal EcoRI cut site was silently mutated using the GLP-1 E27 primers (Table 1). From Fc-GLP-2, we generated site-directed point mutations, specifically changing five acidic amino acids to either neutral, D3Q, or basic, D8K, E9K, N11K, and D15K (referred to as Fc-dipolar GLP-2; Figs. 1 and 2 and Table 1). These mutations were chosen to mimic the dipolar nature of the glucagon  $\alpha$ -helix, which share less than 40% homology, and

## Proglucagon Is Sorted by Dipolar $\alpha$ -Helices

also to keep the  $\alpha$ -helix intact. Finally, each of these constructs was terminated by an in-frame stop codon, introduced either by site-directed mutagenesis or PCR amplification. All results were confirmed by sequencing at the London Regional Genomics Facility, University of Western Ontario.

**Cell Culture and Transient Transfections**—Wild-type PC12 cells (a kind gift from Dr. W. J. Rushlow, University of Western Ontario, London, Ontario, Canada) were maintained in high glucose (25 mM) DMEM (Invitrogen), supplemented with 15% horse serum (Invitrogen) and 2.5% FBS (Invitrogen).  $\alpha$ TC1-6 cells (a kind gift from Dr. C. B. Verchere, University of British Columbia, Vancouver, British Columbia, Canada) were cultured as described previously (34). Cells were transfected using Lipofectamine 2000 (Invitrogen). To prepare cells for microscopy, cells were grown on glass coverslips coated with rat tail type I collagen (100  $\mu$ g/ml; Sigma) at a density of  $4 \cdot 10^5$  cells/cm<sup>2</sup> the day prior to transfection. For secretion assays, cells were grown in poly-D-lysine-coated 6-well tissue culture dishes (Corning Glass). Cells were allowed to grow for 48 h following transfection.

**Secretion Experiments**—On the day of the experiment, media were changed to high glucose DMEM supplemented with 1% dialyzed FBS. After preincubation, cells were incubated for 3 h in the same medium (“3 h basal”) followed by 15-min incubations without (“–K”) and with (“+K”) 55 mM KCl to stimulate granule exocytosis (35). Cells were quickly rinsed in Hanks’ buffered salt solution between incubations. All media (1 ml per sample) were collected on ice, with fresh protease inhibitor mixture (Roche Applied Science), 2  $\mu$ g/ml aprotinin, 55 mM Tris, 1 mM EDTA, pH 7.4, for immunoprecipitation; cell lysates were collected, and protein concentration was quantified as described previously (34).

**Immunoprecipitation, Western Blot, and Secretion Index**—The media and cell lysates were applied to 50  $\mu$ l of protein A-Sepharose (GE Healthcare) and incubated at 4 °C overnight with rotation, after which beads were recovered, and protein was eluted by heating to 70 °C for 10 min. The immunoprecipitated proteins were separated on 10% NuPAGE pre-cast gels (Invitrogen) or SDS-PAGE and transferred to nitrocellulose membranes. Fc-immunoreactive bands were visualized by incubating membranes with goat anti-mouse IgG HRP-conjugated antibody (1:5000 concentration; Invitrogen) followed by SuperSignal chemiluminescent substrate (Thermo-Fisher Scientific, Toronto, Ontario, Canada). Bands were quantified by densitometry as described previously (26). Secretion indexes were expressed as a ratio of stimulated to basal secretion, normalized to total protein (22), and were used for statistical analysis.

**Immunocytochemistry**—Cells were processed for immunocytochemistry as described previously (26). Slides were incubated with antibodies against the secretory granule marker, chromogranin A (CgA) (1:100; Abcam, Cambridge, MA), or the synaptic-like microvesicle marker, synaptophysin (1:250; Abcam). AlexaFluor488 IgG (Invitrogen) was used to visualize the reporter, Fc, and AlexaFluor594 IgG for the CgA or synaptophysin antibody. Coverslips were mounted using a ProLong Gold anti-fade mounting medium (Invitrogen).

**Image Acquisition and Analysis**—Immunofluorescence images were acquired using a Zeiss LSM 510 Duo Vario confocal microscope (Zeiss Canada Inc., Toronto, Ontario, Canada) and a  $\times 63$  1.4 NA Plan-Apochromat oil differential interference contrast objective lens using the Zen 2009 software (Zeiss Canada Inc.). Three coverslips per transfection were imaged for analysis. Image analysis was conducted using FIJI version 1.46h (36), a distribution of ImageJ (National Institutes of Health, Bethesda), using the co-localization 2 plug-in within FIJI. Regions of interest were manually drawn around distinct single or multicell bodies, positive for Fc and either chromogranin A or synaptophysin. Co-localization of these pixels from each pseudo-colored image were used to calculate Pearson’s correlation coefficient, as described previously (33). To generate a three-dimensional rendering of the spatial localization of Fc-WT glucagon and Fc-dipolar GLP-2, the Imaris software package (Bitplane AG, Zurich, Switzerland) was used. The three-dimensional voxel information was used to assign 0.25–0.30- $\mu$ m spheres to computed point sources of light in each channel. Only the co-localized spots are shown, as determined by spatial overlap within a maximum distance of 0.30  $\mu$ m. Correlation coefficients from each experiment were treated as one experimental data set ( $n = 30$ –35).

**Secondary Structure Predictions and Biophysical Property Calculations**—Secondary structure predictions (see Table 2) were carried out with the PSI-PRED algorithm (version 3.1) (37). Percent helical content was calculated as the ratio of total  $\alpha$ -helical residues to the peptide length. The corresponding pI value was calculated using the ExpASY Bioinformatics Portal (38), and the mean hydrophobic moment was calculated using the method of Eisenberg *et al.* (39). Hydrophobic cluster analysis was carried out by the method of Gaboriaud *et al.* (40).

**Statistical Analyses**—Differences were assessed using a one-way analysis of variance with Tukey’s HSD post hoc test. Statistical significance was accepted at the level of  $p < 0.05$ , and the results are expressed as the means  $\pm$  S.E. Statistical analyses were performed using GraphPad Prism version 5.02 (GraphPad Software Inc, La Jolla, CA).

## RESULTS

**Rationale for Using PC12 Cells as a Model of Hormone Trafficking and Secretion**—Although in our previous publication we observed abundant localization of proglucagon in secretory granules in Neuro2a cells (33), these cells did not respond to any secretagogue (K<sup>+</sup>, Ba<sup>2+</sup>, dibutyryl cyclic AMP, and isobutylmethylxanthine alone or in combination) in our hands. Because showing regulated secretion of our fusion constructs was a necessary part of our study, we sought another model of a cell type with a regulated secretory pathway. We avoided the use of  $\alpha$  or L cell lines so as not to confound our results with endogenous proglucagon and derived peptides due to the multistep nature of proglucagon processing. We chose the PC12 neuroendocrine cell line because of the following: 1) They have a very well characterized regulated secretory pathway. 2) They express CPE, which we have shown to be a sorting receptor for proglucagon in  $\alpha$  cells. 3) They lack significant PC1/3 and PC2 activity, thus allowing us to assay individual proglucagon-derived peptides for sorting independently of processing. PC12 cells have

been used to characterize the sorting of multiple classes of neuropeptides and hormones that agree with the mechanism in their native tissues, including the following: proinsulin and proenkephalin (41); pro-brain-derived neurotrophic factor (18, 42); pro-CART (25); pro-neurotensin (43); pro-opiomelanocortin (17); and pro-renin (44). In fact, the regulated secretory pathway in PC12 cells is better characterized than in either of the accepted models of proglucagon processing,  $\alpha$ TC1-6 and GLUTag cells, and they have many key proteins in common. PC12 and  $\alpha$ TC1-6 cells express chromogranin A, and human  $\alpha$  cells additionally express chromogranin B and secretogranins III (34, 45, 46), whereas L cells express CgB and secretogranins II, III, and V (47), thus showing similarities in sorting machinery. The exocytosis machinery is also similar, with both PC12 and  $\alpha$ TC1-6 cells expressing the SNARE proteins syntaxin-1a, VAMP2, SNAP25 (34, 48), and the SNARE-associated proteins Munc13-1 and Munc18-1 (49, 50), whereas AP-1 and AP-3 are expressed by PC12 and mouse  $\alpha$  cells (51). More recently, it has been shown that the GLUTag L cell model also expresses SNAP25, VAMP-1, -2 and -3, syntaxin-1a, and Munc18-1 (52). The literature therefore strongly supports the use of the PC12 cell line as a model for the sorting of proglucagon to the regulated secretory pathway in  $\alpha$  and L cells.

**Glucagon Contains an  $\alpha$ -Helix Sorting Signal**—To identify sorting signals contained within glucagon, we transfected PC12 cells with either Fc alone or the Fc-WT glucagon fusion constructs described in Fig. 2A. Expression of fusion constructs was confirmed by Western blot (Fig. 2B). First, we determined the extent of regulated secretion of fusion proteins from PC12 cells using 55 mM  $K^+$  as a secretagogue. The KCl secretagogue causes depolarization of the plasma membrane, triggering a rapid calcium-dependent fusion of secretory granules with the plasma membrane, resulting in exocytosis of granule cargo. A lack of response to secretagogue stimulation (*i.e.* secretion index equal to unity) indicates constitutive secretion, whereas a significantly elevated secretion index indicates the ability of glucagon to direct Fc into secretory granules of the regulated secretory pathway (53). Second, we examined the extent to which the Fc fusion proteins were sorted to secretory granules by quantitative co-localization with the secretory granule marker, CgA. Taken together, these experiments specifically determined the nature of sorting signals within glucagon that direct it to granules.

As expected, the fragment of the mouse IgG heavy chain, Fc, was secreted in a constitutive manner as shown by the lack of  $K^+$ -stimulated release and a secretion index of 1 (Fig. 3, A and B). In contrast, fusion of Fc to WT glucagon resulted in regulated secretion, as indicated by a robust secretory response to 55 mM  $K^+$  (Fig. 3A) and a secretion index that was significantly elevated ( $p < 0.05$ ) compared with Fc alone (Fig. 3B). Therefore, WT glucagon contains a signal that is sufficient to sort Fc to granules. We then investigated the structural nature of the sorting signal within glucagon by mutating the  $\alpha$ -helix (Fc-LP glucagon) and the role of the  $^{17}RR^{18}$  motif in sorting (Fc-RQ glucagon). The secretion of Fc-LP glucagon secretion did not increase upon secretagogue stimulation (Fig. 3B), and the secretion index was not significantly different from Fc alone (Fig. 3B). In contrast, Fc-RQ glucagon showed similarly regu-

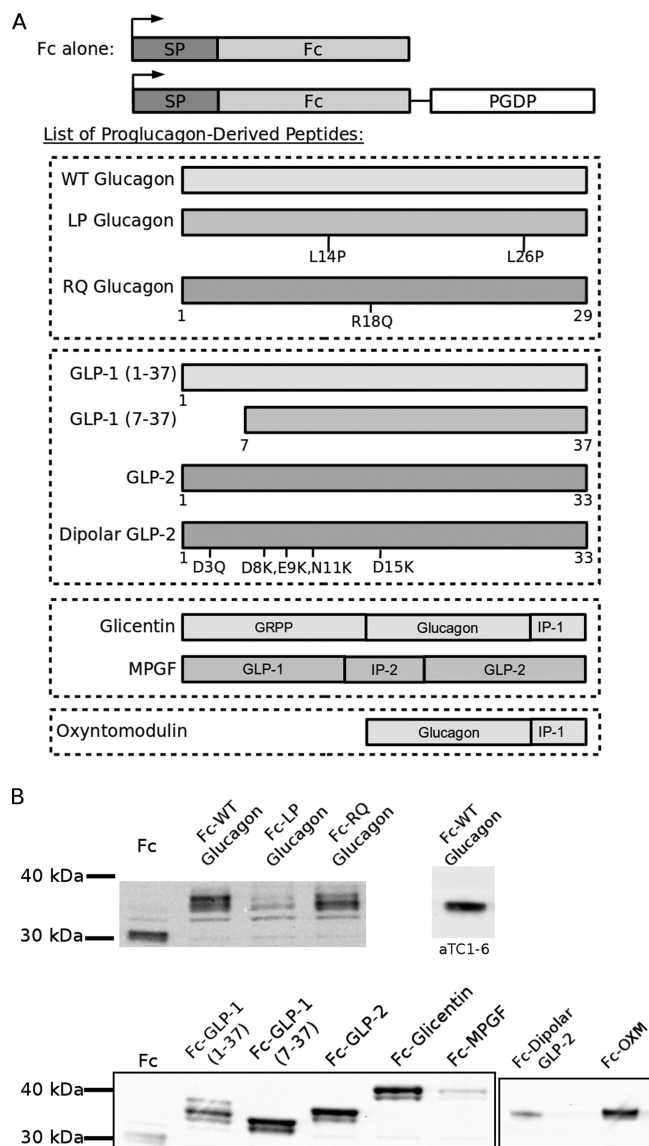


**FIGURE 2. Schematic depiction and expression of fusion proteins.** A, fusion proteins were composed of a signal peptide (SP), mouse IgG-2b heavy chain (Fc), and a proglucagon-derived peptide (PGDP). A control consisted of Fc alone immediately followed by a stop codon. The listed peptides were individually fused in-frame with Fc to generate fusion proteins. Numbers indicate amino acid positions relative to the PGDP sequence. Amino acid mutations and position are indicated within schematic illustration. Dashed boxes indicate the groups of related peptides. Fc-LP glucagon decreases helical content of glucagon, whereas Fc-RQ glucagon changes the dibasic sequence. Fc-dipolar GLP-2 mutations introduce a positively charged surface within the  $\alpha$ -helix to mimic the charge distribution of glucagon/GLP-1. B, expression of fusion proteins in PC12 cells by Western blot. Far right lane shows expression of Fc-WT glucagon in  $\alpha$ TC1-6 cells.

lated secretion to WT glucagon (Fig. 3A) and significantly greater secretion index ( $p < 0.05$ ) compared with Fc alone (Fig. 3B). These results suggest that the  $\alpha$ -helix within glucagon, and not the dibasic site, may serve as a sorting signal to direct proglucagon into granules.

To identify the subcellular distribution of the fusion proteins, we conducted immunofluorescence confocal microscopy to visualize Fc immunoreactivity and the extent of co-localization with the secretory granule marker, CgA. Co-localization was quantified as the fluorescence intensity co-variance between Fc

## Proglucagon Is Sorted by Dipolar $\alpha$ -Helices

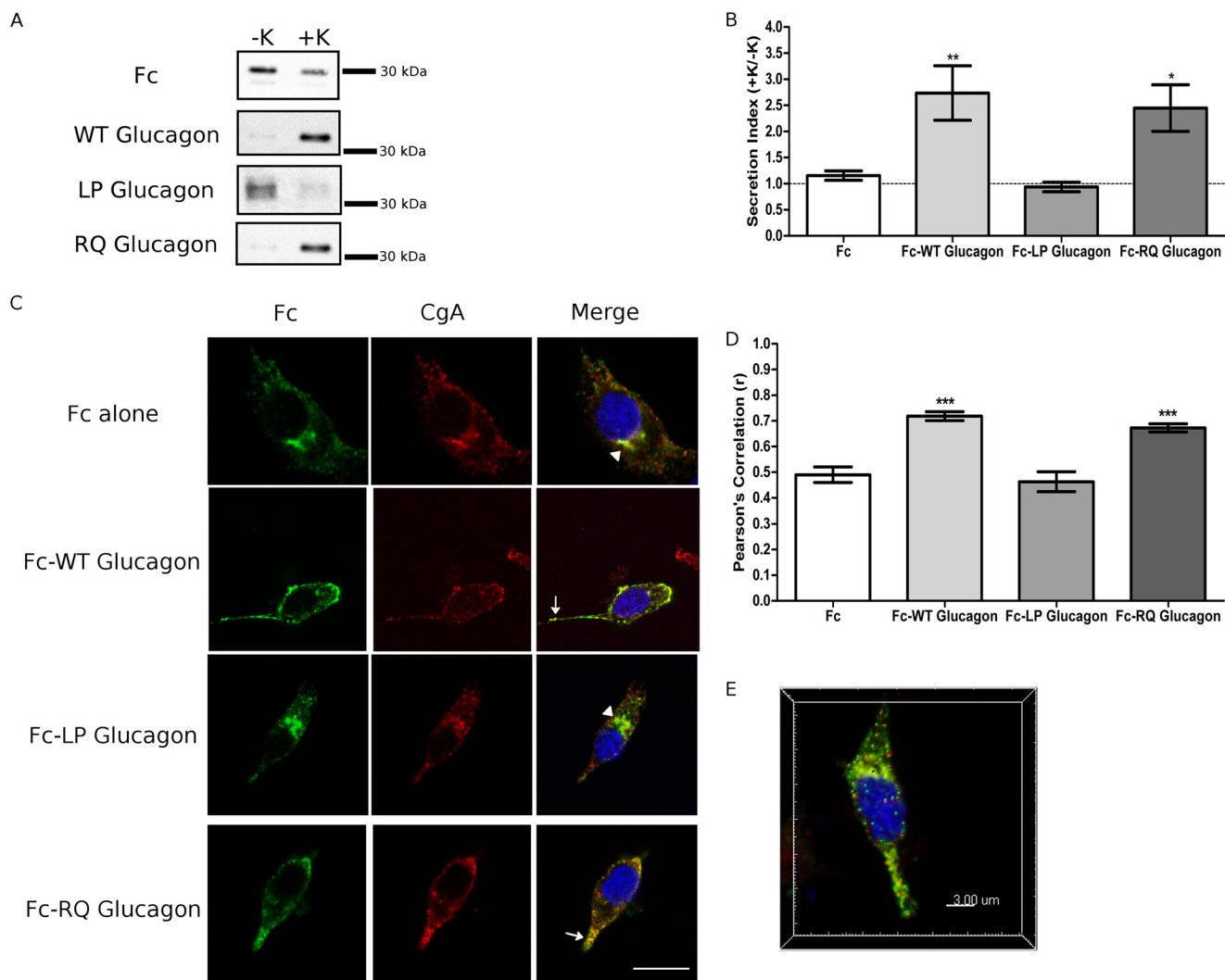


**FIGURE 3. Glucagon contains a necessary  $\alpha$ -helical sorting signal.** PC12 cells were transfected with either Fc alone or Fc-glucagon fusion constructs. *A*, Western blot analysis of regulated secretion. PC12 cells were incubated for 15 min without ( $-K$ ; constitutive) and then with ( $+K$ ; stimulated) 55 mM  $K^+$ . Media were immunoprecipitated for Fc prior to Western blot analysis. Representative blots are shown ( $n = 6$ ). *B*, secretion indexes from *A*. The dashed line indicates a secretion index of unity. Values are means  $\pm$  S.E. ( $n = 6$ ). \*\*,  $p < 0.01$ ; \*,  $p < 0.05$ , versus Fc alone. *C*, subcellular localization of Fc-glucagon fusion proteins. *Arrows* indicate co-localization of Fc with CgA. *Arrowheads* denote Golgi localization. *Scale bar*, 10  $\mu$ m. *D*, PCC for co-localization between Fc and CgA. Values are means  $\pm$  S.E. ( $n = 30-35$ ). \*\*\*,  $p < 0.001$ . *E*, three-dimensional reconstructed volume from confocal stacks of Fc-WT glucagon depicting co-localization between Fc:CgA (translucent yellow) as well as identified spots of co-localization consistent with secretory granules.

and CgA immunofluorescence, using Pearson's correlation coefficient (PCC), as described previously (33). Fc alone had a para-nuclear staining pattern characteristic of Golgi localization (*arrowhead*, Fig. 3C). The corresponding measured fluorescence correlation of Fc and CgA (Fig. 3D) appears high, but it likely reflects the fact that both Fc and CgA are co-trafficked through the Golgi under steady-state conditions, rather than localization of Fc in granules. In contrast, Fc-WT glucagon expression was localized in CgA<sup>+</sup> granules along the cell periphery and toward the tips of the cell processes (*arrow*, Fig. 3C), a pattern that indicates localization in secretory granules (33). Pearson's correlation of Fc-WT glucagon with CgA was significantly greater than Fc alone ( $p < 0.01$ ; Fig. 3D), thus demonstrating the sorting of Fc-WT glucagon to secretory granules. When the  $\alpha$ -helix of glucagon was disrupted in Fc-LP glucagon, Fc immunoreactivity was predominantly localized to the Golgi, and the corresponding Pearson's correlation was not significantly different from Fc alone (Fig. 3D). Finally, Fc-RQ

glucagon was localized within CgA<sup>+</sup> secretory granules in a punctate pattern similar to that of Fc-WT glucagon (*arrow*, Fig. 3C). Pearson's correlation of Fc-RQ glucagon with CgA was significantly greater than Fc alone ( $p < 0.001$ ) (Fig. 3D) and not significantly different from Fc-WT glucagon. Re-construction of the co-localized sub-volume showed similar Pearson's correlation coefficients, and we also show co-localized spots (0.25–0.30  $\mu$ m in size) consistent with secretory granules from the stack (Fig. 3E). Taken together, our results indicate that the  $\alpha$ -helix within glucagon is a necessary and sufficient sorting signal, whereas the dibasic <sup>17</sup>RR<sup>18</sup> motif is not required for sorting.

To show that the sorting of the Fc constructs is not an artifact of the cell type, we repeated secretion and immunofluorescence experiments using Fc-WT glucagon in  $\alpha$ TC1-6 cells, a glucagon-secreting cell line (34). Fc-WT glucagon exhibited a similar degree of stimulated secretion with 15 mM arginine (secretion index (SI) =  $2.3 \pm 0.1$  versus  $1.1 \pm 0.2$  for Fc alone,  $p < 0.01$ ) to

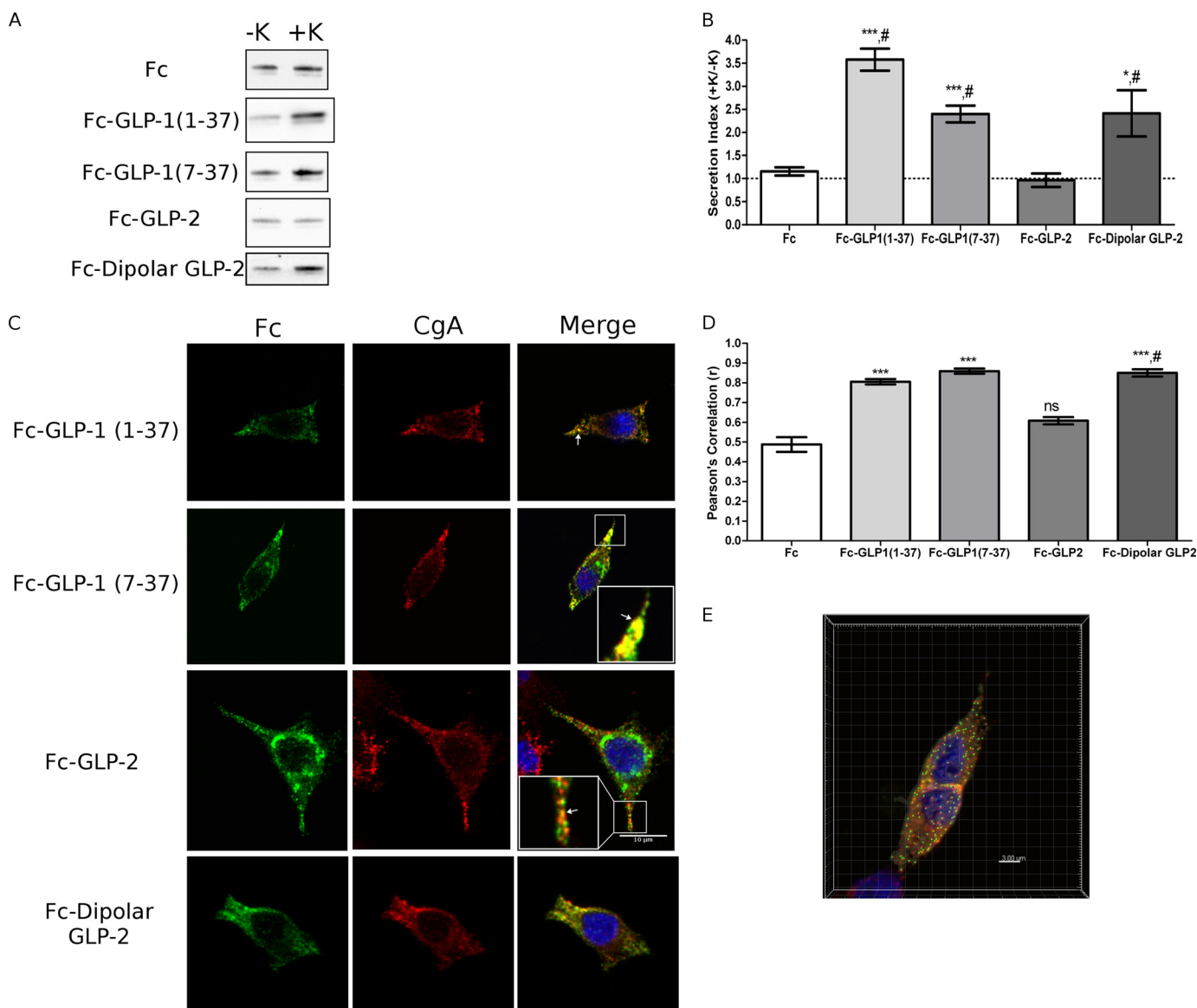


**FIGURE 4. GLP-1 is sorted to secretory granules by a sorting signal within GLP-1(7-37).** PC12 cells were transfected with Fc-GLP-1 or Fc-GLP-2 fusion constructs. *A*, Western blot analysis of regulated secretion. PC12 cells were incubated for 15 min without ( $-K$ ; constitutive) and then with ( $+K$ ; stimulated) 55 mM  $K^+$ . Media were immunoprecipitated for Fc prior to Western blot analysis. Representative blots are shown ( $n = 6$ ). *B*, secretion indexes from *A*. The dashed line indicates a secretion index of unity. Values are means  $\pm$  S.E. ( $n = 6$ ). \*\*\*,  $p < 0.001$  versus Fc alone; #,  $p < 0.001$  versus Fc-GLP-2. *C*, subcellular localization of Fc-GLP-1, Fc-GLP-2, and Fc-dipolar GLP-2 fusion proteins. Arrows indicate co-localization of Fc with CgA. Scale bar, 10  $\mu$ m. *D*, PCC for co-localization between Fc and CgA. Values are means  $\pm$  S.E. ( $n = 30-35$ ). \*\*\*,  $p < 0.001$  versus Fc alone; #,  $p < 0.001$  versus Fc-GLP-2; ns, compared with Fc alone. *E*, three-dimensional reconstructed volume from confocal stacks of Fc-dipolar GLP-2 depicting co-localization between Fc:CgA (translucent yellow), as well as identified spots of co-localization consistent with secretory granules.

that seen in PC12 cells stimulated with 55 mM  $K^+$ . Similar values were also observed in  $\alpha$ TC1-6 cells with the localization of Fc-WT glucagon in CgA $^+$  granules (PCC =  $0.80 \pm 0.03$  versus  $0.51 \pm 0.03$  for Fc alone,  $p < 0.001$ ) as in PC12 cells. As shown in Fig. 2*B*, the level of expression of Fc-WT glucagon in  $\alpha$ TC1-6 cells was within the range observed for PC12 cells. These results validate the use of PC12 cells and Fc-PGDP constructs to identify sorting signals in proglucagon.

**GLP-1, but Not GLP-2, Efficiently Targets Fc to Secretory Granules**—Because our previous work indicated that the processing of proglucagon to glicentin and MPGF may precede entry into granules (33), we tested the possibility that proglucagon may contain sorting signals within its other constituent peptides. Fc fusion proteins of the glucagon-like peptides,

GLP-1 and GLP-2, were constructed and expressed in PC12 cells. Both GLP-1(1-37) and GLP-1(7-37) were included so as to test the role of the N-terminal six amino acids of full-length GLP-1. Both Fc-GLP-1(1-37) ( $p < 0.001$ ) and Fc-GLP-1(7-37) ( $p < 0.001$ ) exhibited robust  $K^+$ -stimulated secretion compared with the constitutively secreted Fc reporter (Fig. 4, *A* and *B*). Surprisingly, Fc-GLP-2 did not exhibit regulated secretion (Fig. 4, *A* and *B*). Immunofluorescence microscopy showed that both forms of Fc-GLP-1 directed Fc to granules, as evidenced by a punctate fluorescence pattern along the cell periphery and toward the tips of cell processes (arrow and inset, Fig. 4*C*). There was significant correlation between CgA and Fc fluorescence for Fc-GLP-1(1-37) ( $p < 0.001$ ) and Fc-GLP-1(7-37) ( $p < 0.001$ ) (Fig. 4*D*). Fc-GLP-2 showed a stronger para-nuclear

## Proglucagon Is Sorted by Dipolar $\alpha$ -Helices

**TABLE 1**

**Primer pairs used for cloning and mutagenesis**

The underlined sequence indicates the restriction sites used for cloning. Boldface sequences indicate site-directed mutations. A conservative mutation was made within GLP-1 to remove an internal EcoRI restriction site. Boldface and underlined text indicates a stop codon.

Fusion construct	Oligonucleotide sequence pair (5' → 3')
Fc (for construction of Fc alone and Fc-glucagon)	Forward, 5'- <u>AAGCTTGGCATGGATCAATT</u> C Reverse, 5'-GGATCCAGGCCTACCCGCAGA
Fc stop mutation	Forward, 5'-GACCATCTCCCGGTCTCCGGGT <b>TAG</b> CCTGGATCC Reverse, 5'-GGACTAGTGGATCCAGG <b>CTA</b> ACCCGGAGACCGGGAG
Fc-glucagon frame shift	Forward, 5'-CCTGGATCCACT <b>C</b> AGTCCAGTGTGGTGG Reverse, 5'-CCACCACACTGGACT <b>G</b> AGTGGATCCAGG
Glucagon <sup>a</sup>	Forward, 5'-GAATTCATTTCACAGGGAACA Reverse, 5'-GCGGCCG <b>CTA</b> GGTGTTCATCAG
L26P-glucagon amplification	Forward, 5'-GAATTCATTTCACAGGGAACA Reverse, 5'-GCGGCCG <b>CTA</b> GGTGTTCATC <b>CGG</b>
R18Q-glucagon mutagenesis	Forward, 5'-AAATACCTGGACTCCCGCCAAGCCCAAGATTTTG Reverse, 5'-CAAAATCTTGGGG <b>TTG</b> CGGGAGTCCAGGTATTT
L14P-glucagon mutagenesis	Forward, 5'-TACAGCAAATACCCGGGACTCCCGCCAGCC Reverse, 5'-GGCTCGCGGGAGT <b>CCGG</b> GTATTTGCTGTA
Fc (for construction with GLP-1, GLP-2, glicentin, MPGF)	Forward, 5'-GCTAGCATGGATCAATTCGGATGG Reverse, 5'-AAGCTTACCCGGAGACCGGGAGATGG
GLP-1(1-37) <sup>b</sup>	Forward, 5'-GGATCCACGATGAGTTTGAGAGG Reverse, 5'-GAATTCCTCTGCCTTTTCACC
GLP-1(7-37) <sup>b</sup>	Forward, 5'-GGATCCACGCTGAAGGGACC Reverse, 5'-GAATTCCTCTGCCTTTTCACC
GLP1 Glu-27 mutagenesis	Forward, 5'-GGCCAGCTGCAAAGGAGTTTCATTGCTTGG Reverse, 5'-CCAAGCAATGA <b>CTC</b> CTTTGCAGCCTGGCC
GLP-1 stop codon mutagenesis	Forward, 5'-GGTGAAGGCAGAGGATGAGAA <b>TTCT</b> GCATATCCTTAAG Reverse, 5'-AAGGATATCTGCAGAA <b>TTCTCA</b> TCTCTGCC TTTCAACCAGC
GLP-2 <sup>b</sup>	Forward, 5'-GGATCCCATGCGGACGGCTCCTTC Reverse, 5'-GAATTCGTCACTGATTTTGGTTTTG
GLP-2 stop codon mutagenesis	Forward, 5'-CAAACCAAATCACTGACTAGGA <b>ATTCT</b> GCAGATATCCTTAAGT Reverse, 5'-AGGATATCTGCAGAA <b>TTCTCA</b> TGTCAGTATTTT GGTTTGAATC
D3Q-GLP-2 mutagenesis	Forward, 5'-GGATCCCATGCGCAGGGCTCCTTCTCC Reverse, 5'-GGAGAAGGAGCC <b>CTG</b> CGCATGGGATCC
D8K,E9K,N11K,D15K GLP-2 mutagenesis	Forward, 5'-GCTCCTTCTCCAAGAAGATGAAGACGATTCTCAAG AGTCTTGCC Reverse, 5'-GGCAAGACT <b>CTT</b> GAGAATCGTCTTCATCT <b>CTT</b> TGGA GAAGGAGC
Glicentin <sup>b</sup>	Forward, 5'-GGATCCATTCCCTTCAGGACACGGAGG Reverse, 5'-GAATTC <b>CTA</b> AGCGTTTGGCAATGTTGTTCTCTGTTT
MPGF <sup>b</sup>	Forward, 5'-GGATCCACGATGAGTTTGAGAGGCAACGC Reverse, 5'-GAATTC <b>CTA</b> TTTCTTGTCACTGATTTTGGTTTGAATCA
Oxyntomodulin <sup>b</sup>	Forward, 5'-CTCGGATCCCATTCACAGGGAACATTCACCACTGACTACAG Reverse, 5'-GTGAATGGGATCCGAGCTCGGTACCAAGCTTACCCG

<sup>a</sup> Constructs used a flexible 10-amino acid linker (sequence GSTQSSVVEF).

<sup>b</sup> Constructs used a flexible 8-amino acid linker (sequence KLGTELGS).

localization and, interestingly, was also present in punctate vesicles that appeared to be distinct from those that were immunopositive for CgA (*arrowhead* and *inset*, Fig. 4C). There was no significant difference in co-localization with CgA and Fc compared with Fc alone (Fig. 4D), consistent with the lack of K<sup>+</sup>-stimulated secretion. Therefore, our data suggest that GLP-1(7-37) contains sufficient information for granule sorting. However, GLP-2 is not sorted efficiently into dense-core secretory granules and may instead be routed to another vesicle compartment in PC12 cells.

**Dipolar  $\alpha$ -Helix GLP-2 Mutant Sorts to Secretory Granules**—Because GLP-2 shares only 38 and 32% homology with glucagon and GLP-1, respectively, it is possible that the sequence context contributes to the differences in the sorting of glucagon and GLP-1 compared with GLP-2. We therefore introduced point mutations in GLP-2 that would mimic the charge distribution within the sequence of glucagon by changing four acidic amino acids in the  $\alpha$ -helix to basic lysines (see “Experimental Procedures” and Table 1), termed “Fc-dipolar GLP-2” (Table 2). In contrast to Fc-GLP-2, Fc-dipolar GLP-2 showed a robust response to 55 mM K<sup>+</sup> (Fig. 5A), and the secretion index was similar to that of Fc-WT glucagon and significantly greater than Fc alone ( $p < 0.05$ ) and Fc-GLP-2 ( $p < 0.05$ ) (Fig. 5B). Immunofluorescence microscopy showed that Fc-dipolar GLP-2 was localized to CgA<sup>+</sup> granules (Fig. 5C). The extent of co-localiza-

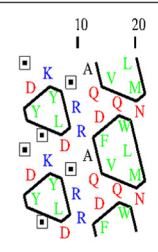
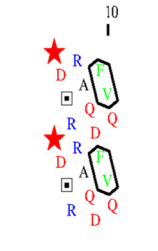
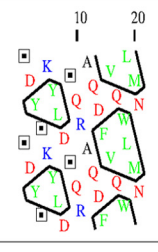
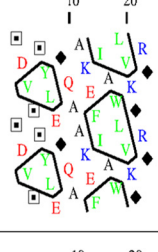
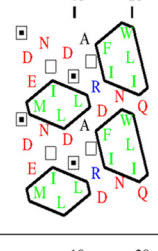
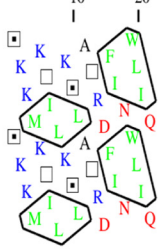
tion between Fc-dipolar GLP-2 and CgA was significantly greater than Fc alone ( $p < 0.001$ ) and WT GLP-2 ( $p < 0.001$ ) (Fig. 5D). Reconstruction of the co-localized sub-volume showed similar Pearson's correlation coefficients (PCC =  $0.78 \pm 0.06$  versus  $0.85 \pm 0.02$ ) and co-localized spots  $0.25\text{--}0.30 \mu\text{m}$  in size from the stack were consistent with localization in secretory granules (Fig. 4E). Therefore, altering the charge distribution of the  $\alpha$ -helix of GLP-2 was sufficient to direct Fc to secretory granules.

**Biophysical Properties of Glucagon, GLP-1, and GLP-2  $\alpha$ -Helices Determine Sorting Efficiency**—Despite the fact that the amino acid sequences of glucagon, GLP-1(7-37), and GLP-2(1-33) are all highly conserved and contain a predominantly  $\alpha$ -helical structure, our results clearly show that the  $\alpha$ -helix alone is not sufficient to target PGDPs to granules. We determined the biophysical nature of the helices by calculating the hydrophobicity and charge distribution for the helical portion of each peptide. The hydrophobic clusters within wild-type glucagon (Table 2 and Fig. 3) were disrupted within Fc-LP glucagon and remained intact in Fc-RQ glucagon, indicating that the leucines are important in the formation of larger hydrophobic clusters. Therefore, the signal within glucagon must consist of an intact  $\alpha$ -helix. We then conducted hydrophobic cluster analysis of glucagon, GLP-1, and GLP-2 and did not observe any differences in either size or location of hydrophobic clusters

**TABLE 2**

**Biophysical properties of major proglucagon-derived peptides**

Amino acid sequences of the peptides used in this study are shown, with the wild-type or mutant sequence indicated. Underlined portions of sequence correspond to  $\alpha$ -helical content of the peptides. Stars indicate proline (hydrophobic); diamonds indicate glycine (uncharged, hydrophobic); open squares indicate threonine (uncharged, polar), and dotted squares indicate serine (uncharged, polar). Enclosed amino acids represent hydrophobic patches.

Fusion Peptide	Peptide Sequence	Mutation	pI	Mean Hydrophobic Moment	Helical Cluster Projection
Fc-WT Glucagon	HSQGTFTSDY <u>SKYLDSRRAQDFVQWLMNT</u> (72% $\alpha$ -helix content)	WT	5.76	0.55	
Fc-LP Glucagon	HSQGTFTSDY <u>SKYPDSRRAQDFVQWPMNT</u> (45% $\alpha$ -helix content)	L14P, L26P	6.39	0.47	
Fc-RQ Glucagon	HSQGTFTSDY <u>SKYLDSRQAQDFVQWLMNT</u> (72% $\alpha$ -helix content)	R18Q	4.43	0.58	
Fc-GLP-1 (7-37)	HAEGTFTSDVSSYLEGQA <u>AKFI</u> AWLVKGRG (68% $\alpha$ -helix content)	WT	4.68	0.69	
Fc-GLP-2	HADGSFSDEMNTILDSL <u>ATRDFINWLIQTKITD</u> (67% $\alpha$ -helix content)	WT	4.23	0.66	
Fc-Dipolar GLP-2	HAQGSFS <u>KKMK</u> TILKSL <u>ATRDFINWLIQTKITD</u> (67% $\alpha$ -helix content)	D3Q, D8K, E9K, N11K, D15K	10.46	0.64	



## Proglucagon Is Sorted by Dipolar $\alpha$ -Helices

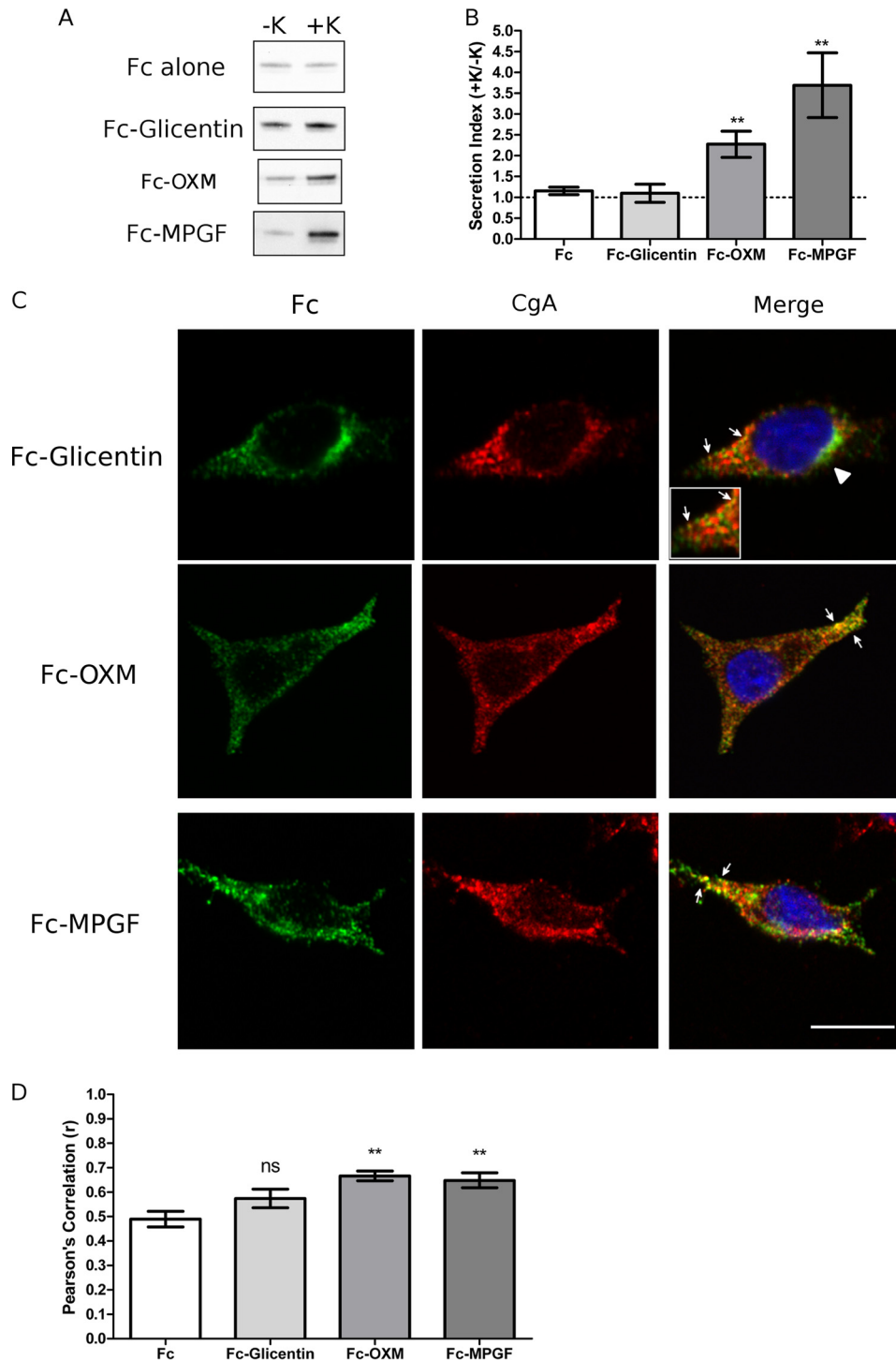


**FIGURE 5. MPGF is efficiently sorted into secretory granules by the sorting signal contained within GLP-1.** PC12 cells were transfected with Fc-glicentin, Fc-MPGF, or Fc-OXM fusion constructs. *A*, Western blot analysis of regulated secretion. PC12 cells were incubated for 15 min without ( $-K$ ; constitutive) and then with ( $+K$ ; stimulated)  $55 \text{ mM K}^+$ . Media were immunoprecipitated for Fc prior to Western blot analysis. Representative blots are shown ( $n = 6$ ). *B*, secretion indexes from *A*. The dashed line indicates a secretion index of unity. Values are means  $\pm$  S.E. ( $n = 6$ ). \*\*,  $p < 0.01$  versus Fc alone. *C*, subcellular localization of Fc-glicentin, Fc-MPGF, and Fc-OXM fusion proteins. Arrows indicate co-localization of Fc with CgA. Arrowheads denote Golgi localization. Scale bar,  $10 \mu\text{m}$ . *D*, PCC for co-localization between Fc and CgA. Values are means  $\pm$  S.E. ( $n = 30\text{--}35$ ). \*\*,  $p < 0.01$  versus Fc alone; ns, compared with Fc alone.

(Table 2) between these highly conserved sequences (54). These  $\alpha$ -helices are flanked by highly conserved N- and C-terminal tails, indicating that these  $\alpha$ -helices are in a similar peptide context. The mean hydrophobic moments for the  $\alpha$ -helix regions of glucagon, GLP-1, and GLP-2 were similar, reflecting the degree of amphiphilicity of these helices. However, there

were significant differences in net charge of the  $\alpha$ -helices. The calculated pI values for the glucagon and GLP-1  $\alpha$ -helices were greater than that of GLP-2 (Table 2), suggesting the net charge (electrical polarization), rather than hydrophobicity, is a more important determinant of proglucagon sorting (Table 2). Finally, based on the charged amino acid distribution, glucagon

and GLP-1 have a net polarization along the length of their helices, and GLP-2 has a more uniform negative charge distribution. By introducing a dipolar mutation to GLP-2, the charge distribution resembled that of glucagon/GLP-1, thus reconstructing a net polarization within GLP-2. Our results demonstrate that efficient targeting of glucagon (Fig. 3), GLP-1 (Fig. 4), and the GLP-2 dipolar mutant (Fig. 4) to granules is determined by dipolar  $\alpha$ -helices, which contain distinct positive and negative patches to polarize the length of the helix, and is sufficient to target glucagon and GLP-1 to secretory granules.

**MPGF, but Not Glicentin, Sorts to Secretory Granules**—It has been documented that initial processing of proglucagon occurs at  $^{70}\text{KR}^{71}$  early in the secretory pathway (5), possibly in the Golgi, to yield glicentin and MPGF (Fig. 1). In this scenario, the processing of proglucagon to glicentin and MPGF may precede sorting to granules. We therefore examined the sorting behavior of glicentin and MPGF with the hypothesis that processing at  $^{70}\text{KR}^{71}$  would occur prior to sorting. Surprisingly, however, secretion of Fc-glicentin was not stimulated by 55 mM  $\text{K}^+$  (Fig. 5A), and its secretion index was similar to Fc alone (Fig. 5B), indicating that glicentin was not sorted to the regulated secretory pathway. In contrast, secretion of Fc-MPGF was significantly stimulated by 55 mM  $\text{K}^+$  ( $p < 0.001$ ) (Fig. 5, A and B). These results were corroborated by analyses of subcellular localization. Fc-glicentin showed very little co-localization with CgA (arrow and inset, Fig. 5C). Quantification of Pearson's correlation coefficients showed Fc-MPGF had a significantly higher value than Fc-glicentin ( $p < 0.01$ ) and Fc alone ( $p < 0.01$ ) (Fig. 5D). Therefore, our data demonstrate that MPGF, but not glicentin, is sorted to granules, thus implying that proglucagon must be sorted to granules prior to being cleaved to glicentin and MPGF. This is an intriguing finding because both glicentin and MPGF contain sorting signals (glucagon and GLP-1, respectively), yet they are sorted quite differently. These results suggest the following: 1) the sorting signal within the sequence of GLP-1 is sufficient to direct MPGF to secretory granules, and 2) the sorting signal within glucagon is masked by the N-terminal GRPP (Fig. 1).

**Oxyntomodulin Sorts to Secretory Granules**—To determine whether GRPP is masking the sorting signal within glucagon, we generated Fc-OXM (Fig. 2). Secretion of Fc-OXM was significantly stimulated by 55 mM  $\text{K}^+$  ( $p < 0.01$ ) (Fig. 5, A and B), in contrast to Fc-glicentin. Immunofluorescence microscopy of Fc-OXM showed co-localization with CgA<sup>+</sup> granules (Fig. 5C), and quantification of Pearson's correlation coefficient showed that Fc-OXM had a significantly greater value than Fc alone ( $p < 0.01$ ; Fig. 5, C and D). Therefore, the sorting signal within glucagon is sufficient to direct oxyntomodulin to granules. These results are consistent with the hypothesis that GRPP masks the glucagon sorting signal in the context of glicentin (Fig. 1), thus providing a mechanism by which glicentin is not sorted to granules.

## DISCUSSION

Highly efficient sorting of proglucagon is required for the maturation of the proglucagon-derived peptides and subsequent storage within secretory granules. Proglucagon is a unique prohormone from the perspective of its structural orga-

nization. Several prohormones, such as pro-thyrotropin-releasing hormone and pro-gonadotropin-releasing hormone, have structured prodomains, whereas the active hormone domain(s) are completely disordered (31). In contrast, proglucagon exhibits disordered prodomains (GRPP, IP-1, and IP-2), with mostly ordered hormone domains, as our previous work has shown (33). Additionally, the sequences of glucagon, GLP-1, and GLP-2 are highly conserved with respect to their charge distribution (32). With this information in hand, we wished to characterize how proglucagon is targeted for regulated secretion by identifying the relevant sorting signals encoded within the ordered hormone domains of proglucagon. We constructed fusion proteins linking each PGDP to a reporter, Fc. Our results demonstrate that both glucagon and GLP-1 contain dipolar  $\alpha$ -helices in which charged residues are distributed around hydrophobic patches and that these helices direct sorting to granules. In contrast, GLP-2, which contains an  $\alpha$ -helix that is not polarized, is very inefficiently sorted. Surprisingly, the sorting of glicentin, which contains the sequence of glucagon and therefore the identified dipolar  $\alpha$ -helix, was inefficient, whereas MPGF maintained its sorting efficiency. Oxyntomodulin was sorted efficiently to secretory granules, thus demonstrating that the N-terminal sequence of glicentin masked the sorting signal contained within the  $\alpha$ -helix of glucagon. We conclude that proglucagon contains two sufficient sorting signals contained within the sequences of glucagon and GLP-1, in the form of a dipolar  $\alpha$ -helix, and that the  $\alpha$ -helix of glucagon is masked after proglucagon is processed to glicentin.

In our previous studies of proglucagon trafficking using Neuro2a cells, our index of sorting efficiency was the co-localization between proglucagon and the cis/medial-Golgi marker, p115 (33). The high correlation value of R18Q-proglucagon led us to conclude that the dibasic  $^{17}\text{RR}^{18}$  sequence within glucagon could contribute to sorting. In this study, we calculated co-localization of the Fc constructs with the granule-resident protein CgA. Here, a high correlation reflected more efficient co-localization in granules, indicating that the  $^{17}\text{RR}^{18}$  sequence may not be a factor in the sorting of proglucagon to granules or that it may be cell type-specific. However, it is important to note that the sorting of the  $\alpha$ -helix mutant of glucagon was calculated to be inefficient in both systems, indicating that the  $\alpha$ -helix within glucagon is a primary sorting signal for proglucagon regardless of the cell type.

Previously identified  $\alpha$ -helical sorting signals indicate that their amphipathic nature directs sorting of prohormones and their processing enzymes to the regulated secretory pathway. Prohormones containing granule-targeting amphipathic helices include pro-somatostatin (24) and pro-CART (25). The sorting signals of the prohormone processing enzymes PC1/3 (53, 55), PC2 (56), and CPE (57) are also amphipathic  $\alpha$ -helices. Our previous work showed that reducing the  $\alpha$ -helical content within glucagon reduced proglucagon sorting efficiency in Neuro2a cells (33). We now show that proglucagon contains two sorting signals in the form of nonamphipathic  $\alpha$ -helices with a unique arrangement of hydrophobic patches and charged residues. Dikeakos *et al.* (27) addressed sorting determinants by using synthetic  $\alpha$ -helices, finding that the tested amphipathic helices with a charged face, or a nonamphipathic

## Proglucagon Is Sorted by Dipolar $\alpha$ -Helices

helix with a substantial hydrophobic patch and segregated charged residues, were efficiently sorted to granules. They inferred two important features of helical sorting signals as follows: segregation of charged residues from hydrophobic patches is essential, and the degree of hydrophobicity correlates well with sorting efficiency. Although synthetic  $\alpha$ -helices were sorted with as few as five charged residues (27), our data showed that as few as three charged residues within the sequences of glucagon and GLP-1 can direct sorting. The pI values of the helices within glucagon and GLP-1 are more similar than GLP-2 to the granule lumen environment, pH 5.5, possibly aiding their targeting to granules. Our hydrophobic cluster analyses show a dipolar charge distribution segregated from hydrophobic patches within glucagon and GLP-1, which were able to sort to granules. In contrast, the helix within GLP-2 has slightly different characteristics; although the nature of the hydrophobic patches is identical to those in glucagon and GLP-1, the charge distribution is not dipolar, consisting of only negatively charged residues along the helix. This difference resulted in very inefficient sorting, suggesting that charge distribution is more important than hydrophobicity for the nonamphipathic  $\alpha$ -helices of proglucagon. We may now estimate the minimal hydrophobic domain required for sorting, in which a large, contiguous hydrophobic face (27) can be reduced to two discontinuous patches of 3 to 4 residues on opposing faces of the helix. This inference is supported by the recent finding that the pro-CART helix contains a smaller hydrophobic face relative to synthetic helices (25). This underscores the importance of the  $\alpha$ -helix as a platform for sorting signal construction in general, and in proglucagon, the sorting information is encoded by the dipolar distribution of electric charge in relation to hydrophobic patches along the helix surface.

The differences in sorting efficiency between glicentin and MPGF suggest a context-dependent regulation of sorting when considering that glicentin does not efficiently sort to granules, despite containing a sorting signal within the sequence of glucagon. After proglucagon is initially processed at the interdomain cleavage site,  $^{70}\text{KR}^{71}$ , glucagon is flanked by the sequences of GRPP and IP-1 (Fig. 1). We used the PSI-PRED server (37) to analyze the predicted secondary structure of glicentin, and it revealed that IP-1 is disordered when not joining glucagon to GLP-1, a characteristic of  $\omega$  loops (58). The N-terminal GRPP domain is also highly disordered and enriched in acidic residues. Our previous model of proglucagon shows this disordered region masks the basic N-terminal residues of the glucagon helix (33), and this study confirms this masking by showing that removal of the GRPP domain results in the targeting of Fc to granules. Conformational masking has been demonstrated in moesin, in which an  $\alpha$ -helical domain regulates the degree of unmasking between its N- and C-terminal ligand-binding domains (59), and in the prohormone protachykinin, in which the negatively charged pro-region masks the positively charged product, calcitonin gene-related peptide (60). We now show that glicentin experiences a similar conformational masking by GRPP. However, MPGF experiences no such masking because IP-2, which links the helices of GLP-1 to GLP-2, appears to be partially helical (5, 33), thus maintaining the availability of the GLP-1 helix for efficient targeting to granules.

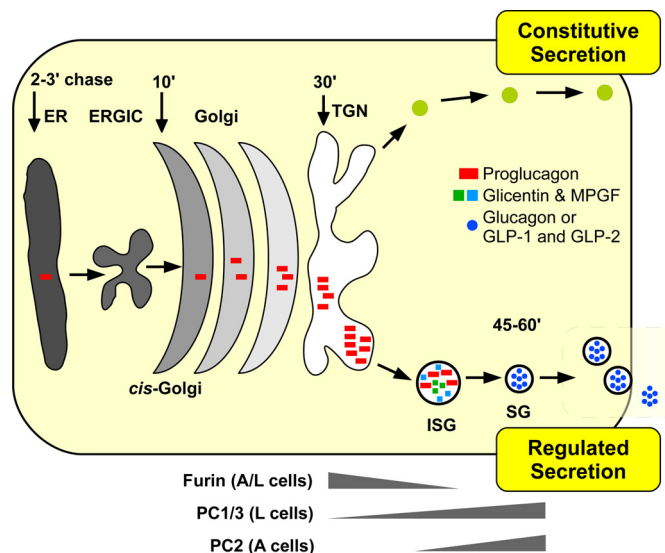


**FIGURE 6. Schematic representation of proglucagon sorting and processing in  $\alpha$  and L cells.** Proglucagon (red bars) is synthesized in the endoplasmic reticulum (ER) and transported through the Golgi to the trans-Golgi network (TGN). Our data support the hypothesis that proglucagon is first sorted to immature secretory granules (ISGs) via dipolar  $\alpha$ -helices within glucagon and GLP-1 and then cleaved to glicentin and MPGF (squares), possibly by furin. Within mature secretory granules (SGs), the prohormone processing enzyme PC2 processes glicentin to glucagon in  $\alpha$  cells, whereas PC1/3 cleaves glicentin and MPGF to yield oxyntomodulin, GLP-1(7–37), and GLP-2 in L cells; ERGIC, ER-Golgi intermediate compartment.

This asymmetry between glicentin and MPGF trafficking presents interesting implications for the temporal relationship between proglucagon processing and sorting. It is well documented that proglucagon processing begins with the early cleavage event at the interdomain site,  $^{70}\text{KR}^{71}$  (5, 9); in  $\alpha\text{TC1-6}$  cells, glicentin and MPGF were detected at 30–45 min via a pulse-chase paradigm (4). Our previous work has shown that mutation of  $^{70}\text{KR}^{71}$  reduced the efficiency of proglucagon sorting in Neuro2a cells (33), and this result led us to conclude that processing may occur before sorting. However, this study does not support this conclusion. If proglucagon processing occurs prior to sorting, our present model would predict that glicentin would be sorted inefficiently, which would impact the production of glucagon in  $\alpha$  cells. Therefore, we now propose that the  $^{70}\text{KR}^{71}$  site simply acts as another sorting signal and, together with the  $\alpha$ -helices of glucagon and GLP-1, targets intact proglucagon to granules, whereupon processing to glicentin and MPGF occurs, as illustrated in Fig. 6. Our model also suggests that the two  $\alpha$ -helical sorting signals are functionally redundant, perhaps reflecting an evolutionary selection toward a high sorting efficiency for proglucagon. That the sequences of glucagon and GLP-1 are highly conserved (32) lends evidence to this reasoning. This is in contrast to pro-thyrotropin-releasing hormone, where PC1/3-mediated processing early in the secretory pathway is required for efficient sorting to distinct subpopulations of granules (61, 62).

Identification of sorting signals within proglucagon gives rise to the question of potential binding partners or sorting receptors. The absence of the processing enzymes PC1/3 and PC2 from PC12 cells supports our previous findings (33) that neither enzyme plays a role in the sorting of full-length proglucagon. The amphipathic  $\alpha$ -helices identified within prohormone-

processing enzymes PC1/3 (26, 63), PC2 (56), and CPE (16) are known to associate with the cholesterol-rich microdomains of granule membranes. However, we could not demonstrate binding of purified proglucagon to liposomes (data not shown) and therefore hypothesize that proglucagon may bind to granule proteins. It is possible that granins bind prohormones, such as pro-opiomelanocortin (64). We have some evidence that proglucagon sorting involves interaction with CPE in  $\alpha$  cells (33). Studies investigating the roles of other granin proteins in sorting proglucagon are currently underway.

In conclusion, we have shown that proglucagon contains two dipolar nonamphipathic  $\alpha$ -helices with relatively small hydrophobic faces that act as sorting signals for entry into secretory granules of endocrine cells. Our data support a mechanism by which proglucagon is sorted to granules prior to the initial cleavage event that results in the production of glicentin and MPGF (Fig. 6). That these sorting domains lie within the ordered domains of encoded proglucagon-derived peptides, and not in a disordered prodomain that characterizes many other prohormones, highlights the unique sorting “signature” of proglucagon and further emphasizes the disparate nature of sorting signals that lie within prohormones and other proteins destined for the secretory granules of the regulated secretory pathway.

*Acknowledgments*—We thank Dr. Jimmy D. Dikeakos (University of Western Ontario) and Dr. Robert B. Mackin (Creighton University, Omaha, NE) for critical reading of the manuscript and Karen Nygard for assistance with confocal microscopy.

## REFERENCES

- Jiang, G., and Zhang, B. B. (2003) Glucagon and regulation of glucose metabolism. *Am. J. Physiol. Endocrinol. Metab.* **284**, E671–E678
- Dong, C. X., and Brubaker, P. L. (2012) Ghrelin, the proglucagon-derived peptides and peptide YY in nutrient homeostasis. *Nat. Rev. Gastroenterol. Hepatol.* **9**, 705–715
- Cohen, M. A., Ellis, S. M., Le Roux, C. W., Batterham, R. L., Park, A., Patterson, M., Frost, G. S., Ghatei, M. A., and Bloom, S. R. (2003) Oxyntomodulin suppresses appetite and reduces food intake in humans. *J. Clin. Endocrinol. Metab.* **88**, 4696–4701
- Rouillé, Y., Westermark, G., Martin, S. K., and Steiner, D. F. (1994) Proglucagon is processed to glucagon by prohormone convertase PC2 in  $\alpha$  TC1-6 cells. *Proc. Natl. Acad. Sci. U.S.A.* **91**, 3242–3246
- Dey, A., Lipkind, G. M., Rouillé, Y., Norrbom, C., Stein, J., Zhang, C., Carroll, R., and Steiner, D. F. (2005) Significance of prohormone convertase 2, PC2, mediated initial cleavage at the proglucagon interdomain site, Lys70-Arg71, to generate glucagon. *Endocrinology* **146**, 713–727
- Furuta, M., Zhou, A., Webb, G., Carroll, R., Ravazzola, M., Orci, L., and Steiner, D. F. (2001) Severe defect in proglucagon processing in islet A-cells of prohormone convertase 2 null mice. *J. Biol. Chem.* **276**, 27197–27202
- Damholt, A. B., Buchan, A. M., Holst, J. J., and Kofod, H. (1999) Proglucagon processing profile in canine L cells expressing endogenous prohormone convertase 1/3 and prohormone convertase 2. *Endocrinology* **140**, 4800–4808
- Dhanvantari, S., and Brubaker, P. L. (1998) Proglucagon processing in an islet cell line: effects of PC1 overexpression and PC2 depletion. *Endocrinology* **139**, 1630–1637
- Dhanvantari, S., Seidah, N. G., and Brubaker, P. L. (1996) Role of prohormone convertases in the tissue-specific processing of proglucagon. *Mol. Endocrinol.* **10**, 342–355
- O'Malley, T. J., Fava, G. E., Zhang, Y., Fonseca, V. A., and Wu, H. (2014) Progressive change of intra-islet GLP-1 production during diabetes development. *Diabetes. Metab. Res. Rev.* **10.1002/dmrr.2534**
- Ravazzola, M., Perrelet, A., Unger, R. H., and Orci, L. (1984) Immunocytochemical characterization of secretory granule maturation in pancreatic A-cells. *Endocrinology* **114**, 481–485
- Noe, B. D., Baste, C. A., and Bauer, G. E. (1977) Studies on proinsulin and proglucagon biosynthesis and conversion at the subcellular level. II. Distribution of radioactive peptide hormones and hormone precursors in subcellular fractions after pulse and pulse-chase incubation of islet tissue. *J. Cell Biol.* **74**, 589–604
- Huang, X. F., and Arvan, P. (1995) Intracellular transport of proinsulin in pancreatic beta-cells. Structural maturation probed by disulfide accessibility. *J. Biol. Chem.* **270**, 20417–20423
- Dhanvantari, S., Shen, F.-S., Adams, T., Snell, C. R., Zhang, C., Mackin, R. B., Morris, S. J., and Loh, Y. P. (2003) Disruption of a receptor-mediated mechanism for intracellular sorting of proinsulin in familial hyperproinsulinemia. *Mol. Endocrinol.* **17**, 1856–1867
- Cool, D. R., Normant, E., Shen, F., Chen, H. C., Pannell, L., Zhang, Y., and Loh, Y. P. (1997) Carboxypeptidase E is a regulated secretory pathway sorting receptor: genetic obliteration leads to endocrine disorders in Cpe(-fat) mice. *Cell* **88**, 73–83
- Zhang, C. F., Snell, C. R., and Loh, Y. P. (1999) Identification of a novel prohormone sorting signal-binding site on carboxypeptidase E, a regulated secretory pathway-sorting receptor. *Mol. Endocrinol.* **13**, 527–536
- Loh, Y. P., Maldonado, A., Zhang, C., Tam, W. H., and Cawley, N. (2002) Mechanism of sorting proopiomelanocortin and proenkephalin to the regulated secretory pathway of neuroendocrine cells. *Ann. N.Y. Acad. Sci.* **971**, 416–425
- Lou, H., Kim, S.-K., Zaitsev, E., Snell, C. R., Lu, B., and Loh, Y. P. (2005) Sorting and activity-dependent secretion of BDNF require interaction of a specific motif with the sorting receptor carboxypeptidase e. *Neuron* **45**, 245–255
- Brakch, N., Allemandou, F., Cavadas, C., Grouzmann, E., and Brunner, H. R. (2002) Dibasic cleavage site is required for sorting to the regulated secretory pathway for both pro- and neuropeptide Y. *J. Neurochem.* **81**, 1166–1175
- Brechler, V., Chu, W. N., Baxter, J. D., Thibault, G., and Reudelhuber, T. L. (1996) A protease processing site is essential for prorenin sorting to the regulated secretory pathway. *J. Biol. Chem.* **271**, 20636–20640
- Bundgaard, J. R., Birkedal, H., and Rehfeld, J. F. (2004) Progastrin is directed to the regulated secretory pathway by synergistically acting basic and acidic motifs. *J. Biol. Chem.* **279**, 5488–5493
- Feliciangeli, S., Kitabgi, P., and Bidard, J. N. (2001) The role of dibasic residues in prohormone sorting to the regulated secretory pathway. A study with proneurotensin. *J. Biol. Chem.* **276**, 6140–6150
- Garcia, A. L., Han, S.-K., Janssen, W. G., Khaing, Z. Z., Ito, T., Glucksman, M. J., Benson, D. L., and Salton, S. R. (2005) A prohormone convertase cleavage site within a predicted  $\alpha$ -helix mediates sorting of the neuronal and endocrine polypeptide VGF into the regulated secretory pathway. *J. Biol. Chem.* **280**, 41595–41608
- Mouchantaf, R., Kumar, U., Sulea, T., and Patel, Y. C. (2001) A conserved  $\alpha$ -helix at the amino terminus of prosomatostatin serves as a sorting signal for the regulated secretory pathway. *J. Biol. Chem.* **276**, 26308–26316
- Blanco, E. H., Lagos, C. F., Andrés, M. E., and Gysling, K. (2013) An amphipathic  $\alpha$ -helix in the prodomain of cocaine and amphetamine regulated secretory peptide precursor serves as its sorting signal to the regulated secretory pathway. *PLoS One* **8**, e59695
- Lacombe, M.-J., Mercure, C., Dikeakos, J. D., and Reudelhuber, T. L. (2005) Modulation of secretory granule-targeting efficiency by cis and trans compounding of sorting signals. *J. Biol. Chem.* **280**, 4803–4807
- Dikeakos, J. D., Lacombe, M.-J., Mercure, C., Mireuta, M., and Reudelhuber, T. L. (2007) A hydrophobic patch in a charged  $\alpha$ -helix is sufficient to target proteins to dense core secretory granules. *J. Biol. Chem.* **282**, 1136–1143
- Sasaki, K., Dockerill, S., Adamiak, D. A., Tickle, I. J., and Blundell, T. (1975) X-ray analysis of glucagon and its relationship to receptor binding. *Nature* **257**, 751–757
- Underwood, C. R., Garibay, P., Knudsen, L. B., Hastrup, S., Peters, G. H.,

- Rudolph, R., and Reedtz-Runge, S. (2010) Crystal structure of glucagon-like peptide-1 in complex with the extracellular domain of the glucagon-like peptide-1 receptor. *J. Biol. Chem.* **285**, 723–730
30. Venneti, K. C., and Hewage, C. M. (2011) Conformational and molecular interaction studies of glucagon-like peptide-2 with its N-terminal extracellular receptor domain. *FEBS Lett.* **585**, 346–352
  31. Dirndorfer, D., Seidel, R. P., Nimrod, G., Miesbauer, M., Ben-Tal, N., Engelhard, M., Zimmermann, R., Winkhofer, K. F., and Tatzelt, J. (2013) The  $\alpha$ -helical structure of prodomains promotes translocation of intrinsically disordered neuropeptide hormones into the endoplasmic reticulum. *J. Biol. Chem.* **288**, 13961–13973
  32. Irwin, D. M. (2001) Molecular evolution of proglucagon. *Regul. Pept.* **98**, 1–12
  33. McGirr, R., Guizzetti, L., and Dhanvantari, S. (2013) The sorting of proglucagon to secretory granules is mediated by carboxypeptidase E and intrinsic sorting signals. *J. Endocrinol.* **217**, 229–240
  34. McGirr, R., Ejbick, C. E., Carter, D. E., Andrews, J. D., Nie, Y., Friedman, T. C., and Dhanvantari, S. (2005) Glucose dependence of the regulated secretory pathway in  $\alpha$ TC1-6 cells. *Endocrinology* **146**, 4514–4523
  35. Taupenot, L. (2007) Analysis of regulated secretion using PC12 cells. *Curr. Protoc. Cell Biol.* Chapter 15, Unit 15.12
  36. Schindelin, J., Arganda-Carreras, I., Frise, E., Kaynig, V., Longair, M., Pietzsch, T., Preibisch, S., Rueden, C., Saalfeld, S., Schmid, B., Tinevez, J.-Y., White, D. J., Hartenstein, V., Eliceiri, K., Tomancak, P., and Cardona, A. (2012) Fiji: an open-source platform for biological-image analysis. *Nat. Methods* **9**, 676–682
  37. McGuffin, L. J., Bryson, K., and Jones, D. T. (2000) The PSIPRED protein structure prediction server. *Bioinformatics* **16**, 404–405
  38. Artimo, P., Jonnalagedda, M., Arnold, K., Baratin, D., Csardi, G., de Castro, E., Duvaud, S., Flegel, V., Fortier, A., Gasteiger, E., Grosdidier, A., Hernandez, C., Ioannidis, V., Kuznetsov, D., Liechti, R., Moretti, S., Mostaguir, K., Redaschi, N., Rossier, G., Xenarios, I., and Stockinger, H. (2012) ExPASy: SIB bioinformatics resource portal. *Nucleic Acids Res.* **40**, W597–W603
  39. Eisenberg, D., Schwarz, E., Komaromy, M., and Wall, R. (1984) Analysis of membrane and surface protein sequences with the hydrophobic moment plot. *J. Mol. Biol.* **179**, 125–142
  40. Gaboriaud, C., Bissery, V., Benchetrit, T., and Mornon, J. P. (1987) Hydrophobic cluster analysis: an efficient new way to compare and analyse amino acid sequences. *FEBS Lett.* **224**, 149–155
  41. Normant, E., and Loh, Y. P. (1998) Depletion of carboxypeptidase E, a regulated secretory pathway sorting receptor, causes misrouting and constitutive secretion of proinsulin and proenkephalin, but not chromogranin A. *Endocrinology* **139**, 2137–2145
  42. Möller, J. C., Krüttgen, A., Heymach, J. V., Jr., Ghori, N., and Shooter, E. M. (1998) Subcellular localization of epitope-tagged neurotrophins in neuroendocrine cells. *J. Neurosci. Res.* **51**, 463–472
  43. Féliciangéli, S., and Kitabgi, P. (2002) Insertion of dibasic residues directs a constitutive protein to the regulated secretory pathway. *Biochem. Biophys. Res. Commun.* **290**, 191–196
  44. Chidgey, M. A., and Harrison, T. M. (1990) Renin is sorted to the regulated secretory pathway in transfected PC12 cells by a mechanism which does not require expression of the pro-peptide. *Eur. J. Biochem.* **190**, 139–144
  45. Stridsberg, M., Grimelius, L., and Portela-Gomes, G. M. (2008) Immunohistochemical staining of human islet cells with region-specific antibodies against secretogranins II and III. *J. Anat.* **212**, 229–234
  46. Hosaka, M., and Watanabe, T. (2010) Secretogranin III: a bridge between core hormone aggregates and the secretory granule membrane. *Endocr. J.* **57**, 275–286
  47. Habib, A. M., Richards, P., Cairns, L. S., Rogers, G. J., Bannon, C. A., Parker, H. E., Morley, T. C., Yeo, G. S., Reimann, F., and Gribble, F. M. (2012) Overlap of endocrine hormone expression in the mouse intestine revealed by transcriptional profiling and flow cytometry. *Endocrinology* **153**, 3054–3065
  48. Wu, Y., Gu, Y., Morphew, M. K., Yao, J., Yeh, F. L., Dong, M., and Chapman, E. R. (2012) All three components of the neuronal SNARE complex contribute to secretory vesicle docking. *J. Cell Biol.* **198**, 323–330
  49. Xia, F., Leung, Y. M., Gaisano, G., Gao, X., Chen, Y., Fox, J. E., Bhattacharjee, A., Wheeler, M. B., Gaisano, H. Y., and Tsushima, R. G. (2007) Targeting of voltage-gated  $K^+$  and  $Ca^{2+}$  channels and soluble N-ethylmaleimide-sensitive factor attachment protein receptor proteins to cholesterol-rich lipid rafts in pancreatic alpha-cells: effects on glucagon stimulus-secretion coupling. *Endocrinology* **148**, 2157–2167
  50. Han, G. A., Malintan, N. T., Collins, B. M., Meunier, F. A., and Sugita, S. (2010) Munc18-1 as a key regulator of neurosecretion. *J. Neurochem.* **115**, 1–10
  51. Sirkis, D. W., Edwards, R. H., and Asensio, C. S. (2013) Widespread dysregulation of peptide hormone release in mice lacking adaptor protein AP-3. *PLoS Genet.* **9**, e1003812
  52. Li, S. K., Zhu, D., Gaisano, H. Y., and Brubaker, P. L. (2014) Role of vesicle-associated membrane protein 2 in exocytosis of glucagon-like peptide-1 from the murine intestinal L cell. *Diabetologia* **54**, 809–818
  53. Jutras, I., Seidah, N. G., and Reudelhuber, T. L. (2000) A predicted  $\alpha$ -helix mediates targeting of the proprotein convertase PC1 to the regulated secretory pathway. *J. Biol. Chem.* **275**, 40337–40343
  54. Seino, S., Welsh, M., Bell, G. I., Chan, S. J., and Steiner, D. F. (1986) Mutations in the guinea pig preproglucagon gene are restricted to a specific portion of the prohormone sequence. *FEBS Lett.* **203**, 25–30
  55. Dikeakos, J. D., Di Lello, P., Lacombe, M.-J., Ghirlando, R., Legault, P., Reudelhuber, T. L., and Omichinski, J. G. (2009) Functional and structural characterization of a dense core secretory granule sorting domain from the PC1/3 protease. *Proc. Natl. Acad. Sci. U.S.A.* **106**, 7408–7413
  56. Assadi, M., Sharpe, J. C., Snell, C., and Loh, Y. P. (2004) The C terminus of prohormone convertase 2 is sufficient and necessary for Raft association and sorting to the regulated secretory pathway. *Biochemistry* **43**, 7798–7807
  57. Dhanvantari, S., Arnaoutova, I., Snell, C. R., Steinbach, P. J., Hammond, K., Caputo, G. A., London, E., and Loh, Y. P. (2002) Carboxypeptidase E, a prohormone sorting receptor, is anchored to secretory granules via a C-terminal transmembrane insertion. *Biochemistry* **41**, 52–60
  58. Fetrow, J. S. (1995) Omega loops: nonregular secondary structures significant in protein function and stability. *FASEB J.* **9**, 708–717
  59. Li, Q., Nance, M. R., Kulikauskas, R., Nyberg, K., Fehon, R., Karplus, P. A., Bretscher, A., and Tesmer, J. J. (2007) Self-masking in an intact ERM-merlin protein: an active role for the central  $\alpha$ -helical domain. *J. Mol. Biol.* **365**, 1446–1459
  60. Ma, G.-Q., Wang, B., Wang, H.-B., Wang, Q., and Bao, L. (2008) Short elements with charged amino acids form clusters to sort protachykinin into large dense-core vesicles. *Traffic* **9**, 2165–2179
  61. Mulcahy, L. R., Vaslet, C. A., and Nillni, E. A. (2005) Prohormone-convertase 1 processing enhances post-Golgi sorting of prothyrotropin-releasing hormone-derived peptides. *J. Biol. Chem.* **280**, 39818–39826
  62. Perello, M., Stuart, R., and Nillni, E. A. (2008) Prothyrotropin-releasing hormone targets its processing products to different vesicles of the secretory pathway. *J. Biol. Chem.* **283**, 19936–19947
  63. Dikeakos, J. D., and Reudelhuber, T. L. (2007) Sending proteins to dense core secretory granules: still a lot to sort out. *J. Cell Biol.* **177**, 191–196
  64. Sun, M., Watanabe, T., Bochimoto, H., Sakai, Y., Torii, S., Takeuchi, T., and Hosaka, M. (2013) Multiple sorting systems for secretory granules ensure the regulated secretion of peptide hormones. *Traffic* **14**, 205–218